Wavenumber Characteristics of a Phase Contrast Interferometer for Waves Propagating Oblique to the Scanning Direction

位相コントラスト干渉計における斜め伝搬波動の波数特性

Takashige TSUKISHIMA*
築 島 隆 繁

Abstract Wavenumber characteristics of a phase contrast interferometer are examined experimentally for ultrasonic waves propagating obliquely to the direction of detector array on the image plane. It is demonstrated that the lower cutoff wavenumber, K_C , increases with increasing the oblique angle, as is expected. It is also found that the value of K_c for the parallel scanning is about one half the value to be expected theoretically.

1. Introduction

The phase contrast interferometer (PCI for short) has been proposed and used [1)-4)] to measure dispersion characteristics of low wavenumber density fluctuations in high temperature plasmas. It makes use of a laser beam which is injected into plasma. When a density wave crosses the laser beam, it behaves like a dynamic grating for laser beam. Hence, the latter is diffracted by the former. The diffracted component is phase-modulated across the beam cross section. Both the phase modulated component and non-modulated zeroth component coming out the plasma together are then passed through an optical system consisting of two convex lenses and a phase plate, and projected on an image plane. This optical system converts the phase modulated component into amplitude modulated one. Thus, when photodiode array is aligned on the image plane along the direction of the wave propagation, the output signals of the phtodiode array represent the propagation characteristic of the density wave.

Extensive studies have been carried out on plasma density fluctuations in fusion devices , using the PCI mentioned above [5)-7)]. In references 4), 6) and 7), effects of oblique density wave propagation with respect to the direction of the laser beam, and finite trasverse dimension of the density wave were considered. In the present report we examine effect of wave propagation oblique to the direction of the photodiode array.

Meanwhile, the PCI has an inherent lower cutoff wavenumber, K_c , below which wave can not be detected. The

* 愛知工業大学 電子工学科（豊田市）

value of K_c depends on several factors, such as diameter of the laser beam, laser wavelength λ, focal length F of the objective lens, and the diameter of the central portion of the phase plate. The zeroth order component of the laser beam passes through the central portion of the phase plate and undergoes a $\lambda/4$ phase shift with respect to the first order diffracted component.

The tranfer properties of the PCI in the low wavenumber regime was well analized theoretically[1], and its validity was confirmed experimentally[3], as well. We have carrid out a simulation experiment making use of ultrasonic wave to generate density wave and found that density wave with a wavenumber of about one half the theoretically predicted cutoff value could be detected with reasonable accuracy.

2. Experimental arrangement

The experimental arrangement is shown schemaitcally in Fig.1. The whole optical system is mounted on an 90 cm ×180 cm optical bench. A He-Ne laser oscilator launches a Gaussian beam having a wave length of 632.8 nm and a beam waist of about 0.5 mm. It is once reflected by the mirror M_1 and then goes through the beam expander BX where the narrow beam is expanded to a wide beam with a waist of w_o = 4.2 mm. At the exit of BS , a Ultrasonic wave having a transverse dimension of about 10 mm propagates across the laser beam perperndicularly.

The image of the ultrasonic wave is transfered by the optical system on vertual image plane where photodiode detectors are located. The optical system consists essentially of two convex lenses L_1 , L_2 , and a phase plate PP, besides relay mirrors M_2 and M_3 and beam splitter BS which allows for two signals at diferent spatial positions to be detected simultaneously. The detector D_1 is located at a fixed position and provide a reference sig-

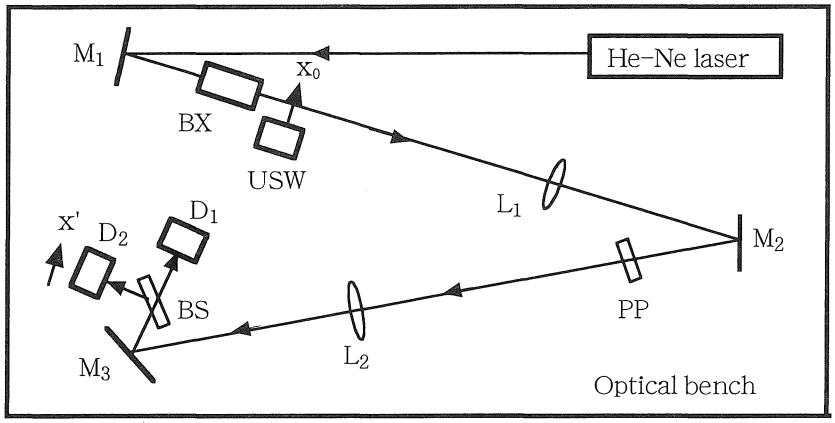

Fig. 1. Experimental arrangement . M_1～M_3 : mirrors, L_1,L_2: lenses, BX: beam expander, USW: ultrasonic wave launcher, PP: phase plate, BS: beam splitter, and D_1,D_2: photodiode detectors.

nal, while the detector D_2 is scanned along a horizontal direction x'.

The function of the phase plate is best understood by refering to Fig.2 which explanes the principle of the PCI. A ultrasonic wave having a wavenumber K is launched along the object plane. The first order laser beam diffracted by the ultrasonic wave is focusd on the focal plane at a position $x=(F/k)K$ distant from the center, while the zeroth order beam is focused at the center of the focal plane. The size of the central portion where the zeroth order beam undergoes the $\lambda/4$ phase shift is $2x_c$. Both the zeroth order component and the first oder deffracted component are superposed on the image plane via the imaging lens L_2 to form an image of the density wave. Hence it is obvious that the density wave with K less than K_c can not be detected, where K_c is defined by

$$K_c \equiv (kx_c)/F , \qquad (2.1)$$

$k=2\pi/\lambda$ is the wavenumber of the laser light , and F is the focal length of the lenses L_1 and L_2 . In the present experiment, we chose F=80 cm and x_c =168 μm. No smaller than this value for x_c was possible because of fabrication limit.

The oblique propagation of the ultrasonic wave is realized by turning the ultrasonic wave launcher around

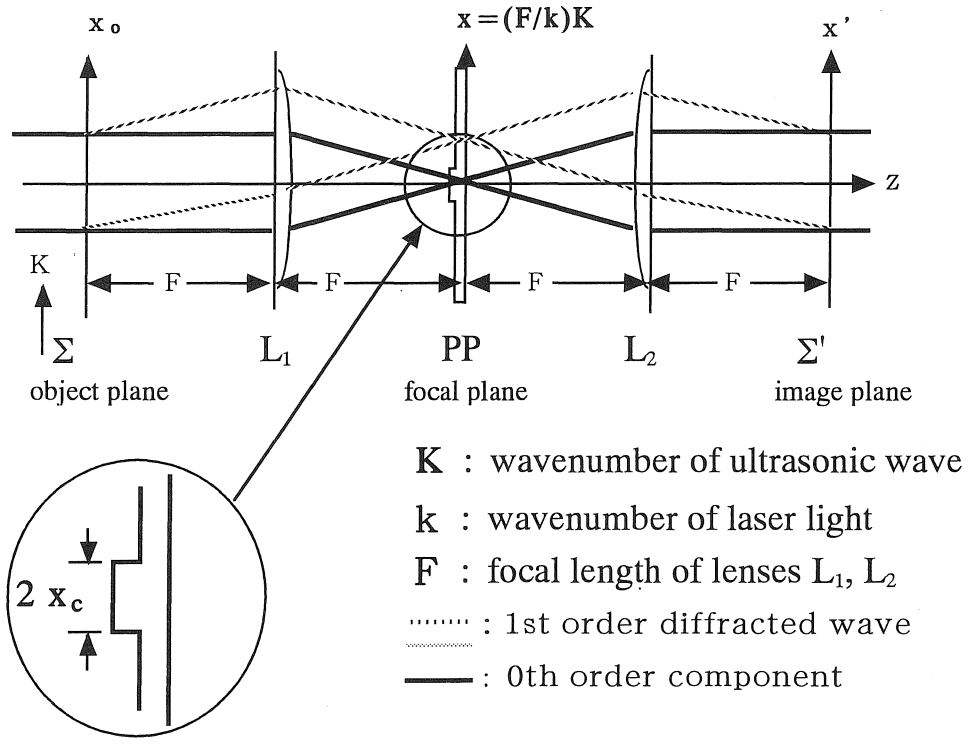

Fig. 2. Optical configuration of the phase contrast interferometer

the laser beam axis, as schematically shown in Fig.3.

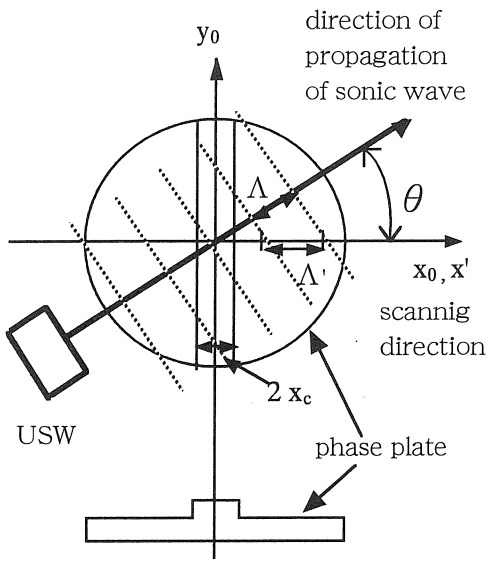

Fig.3. Oblique propagation of sonic wave against scanning direction.

When the ultrasonic wave propagates at an angle θ with respect to the scanning direction , or the direction of the diode array, the wavelength Λ' to be measured by the PCI is given by,

$$\Lambda' = \Lambda / \cos\theta \ , \qquad (2.2)$$

where $\Lambda = 2\pi/K$. In terms of wavelength, Eq.(2.1) is rewritten as,

$$\Lambda_c = F/(x_c \lambda). \qquad (2.3)$$

When Λ' exceeds Λ_c , the wave signal fails to be detected. This is equivalent to saying that the effective cutoff wavenumber K'_c increases with incresing θ , such that,

$$K'_c = (kx_c)/F\cos\theta \ . \qquad (2.4)$$

3. Data acquisition and processing

Let the wave signals detected by the Photodiodes D_1 and D_2 be $S_1(x_1,t_1)$ and $S_2(x_2,t_2)$, respectively. Note that the notations x'_1 and x'_2 are replaced by x_1 and x_2 for simplicity. These two signals are simultaneously recorded on a two channel digital oscilloscope and transfered to a personal computer. The record length for one channel is 2000 points, and the full scale amplitude is digitized in 256 steps.

The cross correlation $R_{12}(x, \tau)$ of the two signals is computed on the PC for varying values of x and τ , according to Eq.(3.1).

$$R_{12}(x,\tau) = \frac{1}{T}\int_0^{T-\tau} S_1(x_1,t_1) S_2(x_2,t_1+\tau)\, dt_1 \qquad (3.1)$$

where $x_2 = x_1 + x$.

$R_{12}(x, \tau)$, as a function of τ, yields the same oscillatory signal as the sonic wave for a given value of x. For different value of x, say $x+\Delta x$, a phase shift of $\Delta\phi$ is introduced, which can be expressed as,

$$\Delta\phi = K\,\Delta x = 2\pi f \Delta\tau \ , \qquad (3.2)$$

where f is the frequency of the ultrasonic wave. The phase verlocity V_x of the density wave along the scanning direction is obtained from a τ vs. x plot. Knowing the value of f , corresponding value of wavelength Λ, or wavenumber K is obtained.

In the experiment, $R_{12}(x, \tau)$'s are calculated for varying values of x, in steps of 0.3 mm, and for varying val

ues of θ in steps of 10 deg.

4. Experimental results

Figure 4 shows a typical τ vs. x plot for f=196.1 kHz and $\theta=0$. The straight line drawn in Fig.4 indicates the least square fitting of the experimental data. The gradient A of this line yields the phase velocity of $V_x=1/A=346.02$ m/s. The phase velocity calculated from the wellknown formula,

$$V=331.53+0.61\,T(℃)\ \text{m/s}, \qquad (4.1)$$

gives V=345.53 m/s for T=23 ℃. The discrepancy between the two values is accounted for by an offset angle $\Delta\theta=\cos^{-1}(V/V_x)=-3.05$ deg.

Another example of the τ vs. x plot is shown in Fig.5 for f=40.82 kHz and $\theta=0$. In this example, the discrepancy between V and V_x is beyond the offset correction. In addition, a considerable deviation of the data from the least square-fitted line is observed. As a measure of bad fitting, the variance

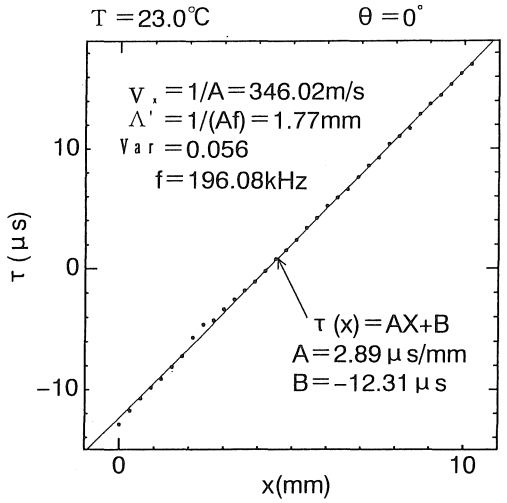

Fig. 4. Propagation characteristic of ultrasonic wave. f=198.1 kHz , $\theta=0$.

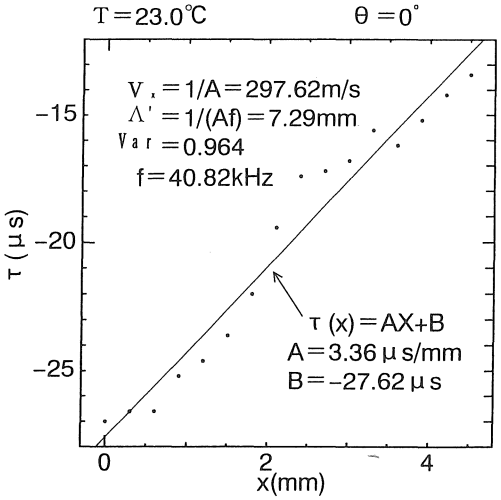

Fig. 5. Propagation characteristic of ultrasonic wave. f=40.82 kHz , $\theta=0$.

Var. defined by Eq.(4.2) is calculated.

$$Var \equiv \frac{1}{n}\sum_{i=0}^{n}\{\tau_i-\tau(x_i)\}^2 \qquad (4.2)$$

Figures 6(a), 6(b), and 6(c) show the values of Λ' and Var as functions of θ, for different sonic frequencies of 198.1 kHz , 71.43 kHz, and 40.82 kHz, respectively. In these figures, the solid curve smoothly connecting dots represent the measured values, while the dotted curves connecting circles stand for calculated ones afterEq. (2.2).

It is interesting to note that the measured values of Λ' for f=196.1 kHz shown in Fig. 6(a) coincide pretty well with the calculated ones even for $\theta=60$ deg. where they exceed the cutoff value Λ_c. The variance is also small for f=196.1 kHz. It is about 0.1 at the maximum.

For f=40.82 kHz shown in Fig. 6(c), the theoretical value of Λ' is already well above the cutoff value, and the measured values of Λ' deviate

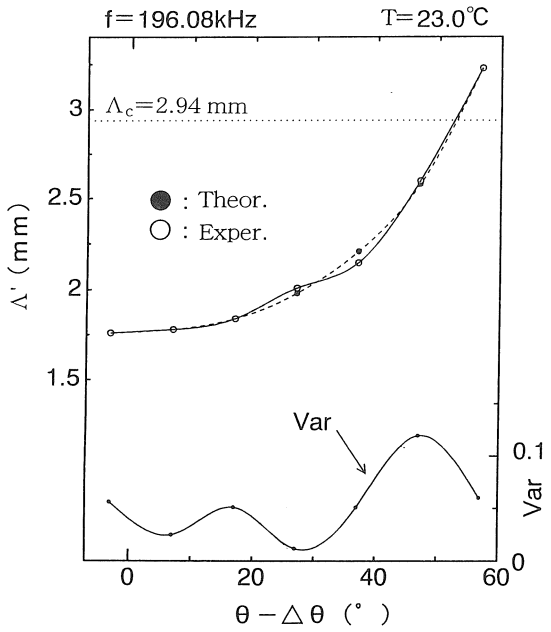

Fig. 6(a). Wavelength Λ' and variance Var vs. θ for f=196.1 kHz.

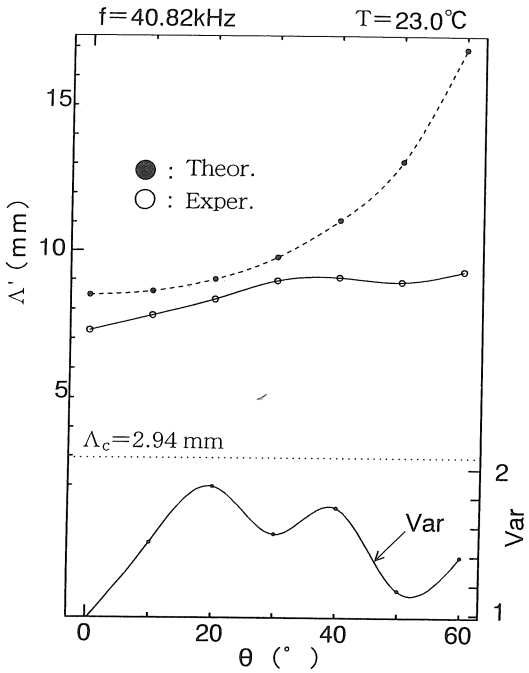

Fig. 6(c). Wavelength Λ' and variance Var vs. θ for f=40.82 kHz.

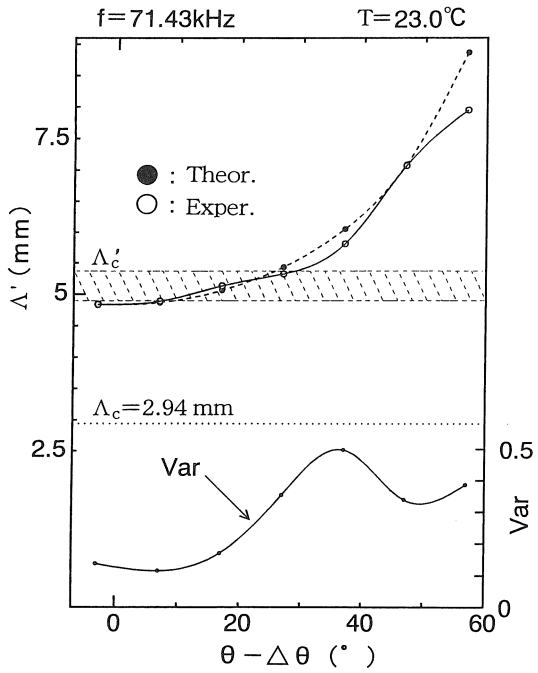

Fig. 6(b). Wavelength Λ' and variance Var vs. θ for f=71.4 kHz.

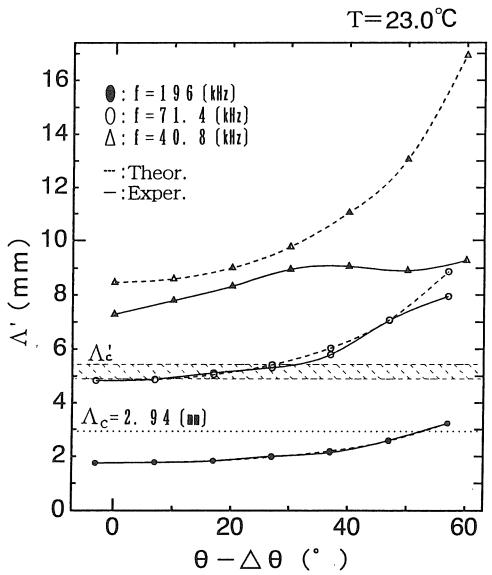

Fig.7. Summary of data for three ultrsonic waves with different frequencies, f=196.1 kHz, f=71.4 kHz, and f=40.82 kHz.

from the calculated ones with increasing θ . The variance is also considerable for all θ .

Figure 6(b) for f=71.34 kHz shows an intermediate case between Fig. 6(a) and Fig. 6(c). The value of Λ' is already about twice the cutoff value for $\theta=0$. Nevertheless , the agreement between measured and calculated values of Λ' is good, and the variance is also small, i.e. Var$\fallingdotseq$0.1. With increasing θ , however, both the discrepancy of Λ's and the value of Var grow. It appear that a critical point exists around $\theta=30$ deg. , over which the difference and variance become appreciable.

Figure 7 summarize whole experimental results : the values of Λ' for the three different frequencies are plotted on the same scale so that relative significance becomes clear. The experimental and theoretical values of cutoff wavelength Λ'_c and Λ_c are also shown in the figure.

5. Discussions and conclusions

There are several factors which affect K_c, as mentioned in Chap.1. The theoretical expression Eq.(2.1) assumes that the waist w_f of the zeroth component of the laser beam on the focal plane is less than x_c , i.e.,

$$w_f < x_c , \qquad (5.1)$$

Meanwhile, the value of w_f for the present Gaussian beam is given by,[9]

$$w_f = \lambda F/(\pi w_o). \qquad (5.2)$$

For our experimental value of F=800 mm, $\lambda=632.8$ nm, and $w_o=4.2$ mm, we have $w_f=38.4$ μm which satisfies the condition Eq.(5.1).

Meanwhile, the cross section of the central portion of the phase plate, where the laser beam experience the $\lambda/4$ phase shift, is shown by a box in Fig. 2. The actual cross section, however, was more or less like a trapezoid with a top width of 285 μm and the average width of $2x_c=336$ μm.

The diffused edge of about 25 μm thickness and the finite spot size of the focal point mentioned above may affect the wavenumber characeristic around the cutoff value K_c . In fact, a detailed analysis has beeen carried out for the case with finite spot size or for the input laser beam with finite transverse dimension by Weisen.[1] We followed his method of analysis and made a numerical calculation on wave number transfer characteristc using our experimental parameters. A result for $x_c=160$ μm and $w_o=4.2$ mm is shown in Fig. 8.

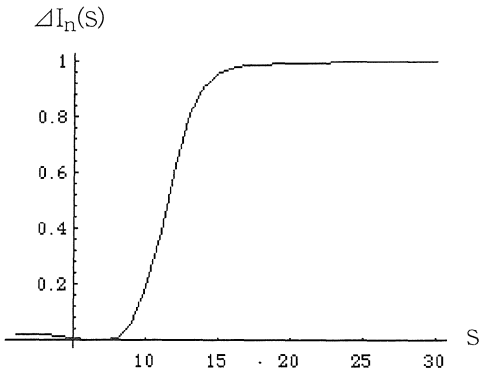

Fig. 8. Normalized transfer function $\Delta I_n(S)$ vs. S, where S is integer and related to K by $K=2\pi(S-1)\Delta k$ with $\Delta k=1/32$ mm^{-1} .

We have confirmed that the value of K for which the normalized transfer function takes a value of 0.5 in Fig. 8 corresponds to K_c defined by Eq.(2.1).

It would be difficult to imagine from Fig. 8 that the density wave with $K \fallingdotseq 0.5 K_c$ could be detected. In other words, the experimental evidence that the measured cutoff wavenumber is about one half the theoretical value given by Eq.(2.1) is hard to be explained theoretically, even if the effect of the diffused edge of the phase shifter is taken into considerations.

As for the oblique propagation characteristics, the experimental results are quite consistent with theoretical predictions, except for the cutoff problem: both the apparent wavelength and the variance increase with increasing angle of wave propagation with respect to the scanning direction of the detector. It is mentioned that turning the USW launcher around the laser beam axis is equivalent to turning the phase plate, provided the phase shifter is of line shape as depicted in Fig. 3.

Acknowledgements

The author would like to appreciate the collaborations of many undergraduate students who conducted research works for bachelors thesis under his supervision during 1994 through 1997. Special thanks are due to T. Yamada who completed software for data acquisition and processing, to T.Sato and T.Sonoda who took pains of repeating many measurements under different conditions.

References

1) H. Weisen : " Imaging Methods for the Observation of Plasma Density Fluctuations ", Plasma Phys. Controlled Fusion, Vol. 28, No.8, pp.1147-1159, Aug.1986.

2) H. Weisen, Ch. Hollenstein and R.Behn : " Turburent density fluctuations in the TCA Tokamak ", Plasma Phys. Controlled Fusion, Vol. 30, No.3 pp.293-309, Mar.1988.

3) H. Weisen : " The phase contrast method as an imaging diagnostic for plasma density fluctuations ", Rev. Sci. Instrum. Vol. 59, No.8, pp.1544-1549, Aug.1988.

4) K. Matsuo, K. Tanaka, K. Muraoka and M. Akazaki : " Development of laser electron density fluctuations ", Jpn. J. Appl. Phys. Vol. 30, No.3, pp.1102-1108, May 1991.

5) S. Coda and M. Porkolab : " A phase contrast interferometer on DIII-D ", Rev. Sci. Instrum. Vol. 63, No.10, pp.4974-4976, Oct.1992.

6) K. Tanaka, K. Matsuo, K. Goto, M. Bowden, K. Muraoka, T. Furukawa, S. Sudo, and T. Obiki : " Applicability of laser phase contrast method for the measurements of electron density fluctuations in high-temperature plasma ", Vol. 31, No.7, pp.2260-2262, Part 1, Jul.1992.

7) K. Tanaka, K. Matsuo, S. Koda, M. Bowden, K. Muraoka, K. Kondo, T. Furukawa, F. Sano, H. Zushi, T. Mizuuchi, S. Besshou, H. Okada, K. Nagasaki, M. Wakatani, T. Obiki and S. Sudo : " Characteristics of electron density fluctuations in Heliotron E measured using a wide beam laser phase contrast method ", J. Phys. Soc. Jpn, Vol. 62, No.9, pp.3092-3105, Sep. 1993.

8) K. Tanaka : " Development of laser phase contrast interferometer and its application to electron density measurements in a high temperature plasma ", Ph.D. thesis (in Japanese), 1995.

9) K. Iizuka, Engineering Optics, 2nd ed. Springer-Verlag, Berlin, 1986, p.150.

（受理　平成 9 年 3 月21日）